Int. J. Anal. Appl. (2025), 23:82

International Journal of Analysis and Applications

Improving Computer Experiment Designs with Two-Type Marked Point Processes

Hichem Elmossaoui*, Ahmed Ait Ameur, Nadia Oukid

LAMDA-RO Laboratory, Department of Mathematics, Faculty of Sciences, University Saad Dahlab Blida 1, BP 270 Soumâa, Blida, Algeria

*Corresponding author: elmossaoui.hichem@yahoo.com

Abstract. This paper presents an alternative approach to constructing computer experiment designs based on stochastic process theory, specifically marked point processes with two types. The originality of this method lies in the use of Markov Chain Monte Carlo (MCMC) techniques, combined with the Metropolis-Hastings algorithm and a new dynamic called local shift dynamics. These tools enable the generation of highly flexible and adaptable experimental designs, which can be tailored to a variety of specific objectives according to experimental needs. Special attention has been given to analyzing the convergence of the Markov chain, thus ensuring the robustness and efficiency of the results obtained. Additionally, a comparative study was conducted to position our method relative to other existing computer designs. This comparison highlights the advantages and disadvantages of our approach in terms of modularity and performance.

1. Introduction

In an increasingly digital world, computer experiment designs play a crucial role in simulating situations, analyzing data, and making informed decisions in various fields, including scientific research and business management. These methodologies foster innovation and enhance our understanding of complex phenomena. In the context of numerical simulation, where experiments can be computationally expensive, it is essential to use experimental design methods to optimize their planning. Numerical models, consisting of simulation codes, connect descriptive variables of the system's state to specific parameters; however, these calculations often remain complex and time-consuming to execute. To address this issue, it is advisable to replace the simulator with approximation functions, built from interpolation methods and computer experiment designs, which can save time and improve the efficiency of simulations.

Received: Jan. 5, 2025.

2020 *Mathematics Subject Classification.* 05B30, 60G55, 62K99.

Key words and phrases. experiment designs; computer experiment designs; point processes; Marked point processes; Markov chain Monte Carlo (MCMC) method; Metropolis-Hastings algorithm.

https://doi.org/10.28924/2291-8639-23-2025-82
ISSN: 2291-8639

To optimize the exploration of experimental parameters and gather relevant information across the entire experimental domain, we propose an innovative method for computer experiment designs. The main goal is to ensure that experiments are distributed as uniformly as possible within the unit hypercube, ensuring consistent coverage of the search space. This approach not only maximizes the efficiency of parameter exploration but also improves the accuracy of the obtained results. To achieve this, we rely on the use of a point process that generates the points forming the experiment designs. This process is defined according to a Markovian structure, in line with Ripley-Kelly's interpretation [1]. The Markovian nature of the process ensures that each point is generated considering the others. This method is distinguished by its ability to reduce redundancy in experiments while effectively covering the parameter space.

In 2008, Franco [2] first introduced an innovative approach to the computer experiment designs, based on the Strauss point process. This process incorporates the concept of pairwise point interaction, adding an extra dimension to the spatial distribution of data. In 2020, Elmossaoui et al. [3, 4] expanded this field by proposing a method based on the marked Strauss process. This approach allowed for the optimization of both the distribution of points in space and the characterization of the marks associated with these points. Recently, in 2023 and 2024, Elmossaoui et *al.* further advanced the research by developing a method for constructing computer designs based on the connectivity interaction and area-interaction point process [5, 6] . This method establishes links between points and analyzes their complex interactions.

Our approach stands out by going even further: we use a marked point process, introducing two distinct marks [7]. To create these designs, we rely on advanced simulation techniques, particularly Markov Chain Monte Carlo (MCMC) methods and the Metropolis-Hastings algorithm [8]. These sophisticated tools allow for the generation of computer experimental designs with a high degree of precision and flexibility. Thus, the evolution of these methods reflects a continuous effort to optimize computer designs, gradually integrating interaction and connectivity elements while leveraging increasingly efficient simulation techniques.

2. Preliminaries

Let $(\Omega, \mathcal{A}, \mathcal{P})$ be a probability space. Consider χ as a non-empty set equipped with the Euclidean distance d, which makes it a complete separable metric space. If we assume that the model has p continuous factors of interest, where $p \geq 1$, then in most cases, χ will be equal to $[0,1]^p$ (a subset of $\mathbb{R}^p$).

Definition 2.1. *A configuration is defined as a countable set, unordered set of points $x = (x_1, x_2, ..., x_n)$, where $x_i \in (\chi, d)$, representing the points resulting from a random experiment. A configuration is said to be locally finite if it contains at most a finite number of points within any bounded Borel set A in (χ, d). We denote N^{lf} as the family of locally finite configurations.*

Definition 2.2. *A point process is a mapping X from a probability space (comprising a metric space χ equipped with a sigma-algebra $\mathcal{A}$ and a probability measure $\mathcal{P}$) to the family of locally finite configurations*

of points in χ. This mapping satisfies the property that for any Borel set $A \subseteq \chi$, the number of points in A, denoted by $N_X(A)$, is a finite discrete random variable.

Definition 2.3. *A marked point process is a random sequence $X = \{x_n, m_n\}$ consisting of a point process x_n defined on (χ, d) and corresponding marks m_n for each x_n in a mark space $\mathcal{M} = (K, d')$.*

Figure 1 represents an example of a marked point process with two marks.

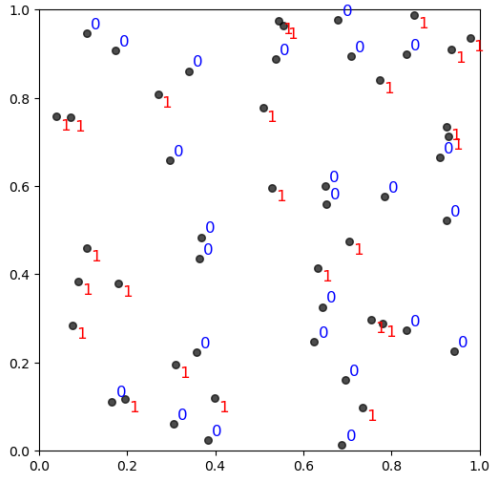

FIGURE 1. Example of a marked point process with two marks.

3. Computer Experimental Design Using Marked Markovian Strauss Point Processes

The main idea is to consider each experiment x_i as a point or particle defined within $[0,1]^p$, and each configuration x as a matrix of experiments. Each point in this configuration is characterized by two marks m_i and m_i' defined in the mark space $\mathcal{M}$. The point and its marks form an object defined as $\left(x_i, m_i, m_i'\right)$. Therefore, we equate the objects (experiment design) to realizations of the two-marked point process X. The marked process implies the possibility of interaction. These interactions correspond to neighborhood properties defined in the Ripley-Kelly [1] Markov field. The most commonly used interaction potential is the interaction between pairs of objects. These object processes are crucial for modeling repulsive phenomena. The probability density of a two-marked point process for a configuration x of points is given by:

$$\pi(x) = \alpha \beta_1^{m_1(x)} \beta_2^{m_2(x)} \gamma_{11}^{m_{11}(x)} \gamma_{12}^{m_{12}(x)} \gamma_{22}^{m_{22}(x)} \tag{3.1}$$

Where,

- α is the normalization constant,
- $0 < \gamma_{kl} \leq 1$, where $k \in \{1,2\}$ and $l \in \{1,2\}$ are interaction coefficients,
- β_k, where $k \in \{1,2\}$, is the intensity of the process,
- $m_k(x)$ is the number of points with mark k in x,
- $m_{kl}(x)$ is the number of pairs of $\sim_x$-neighbors of type (k,l) or (l,k) in x (both marked as k and l simultaneously).

3.1. **Mark Selection.** In this study, we characterize the points using two marks: the first one will be the value of the prediction error $\hat{y}_{x_i}$ at point x_i. Recall that this value is defined as [2]:

$$\text{Var}\left(\hat{y}_{x_i}\right) = {}^t f\left(x_i\right)\left({}^t XX\right)^{-1} f\left(x_i\right)$$

Where,

- $X = {}^t\left[f(x_1), f(x_2), \ldots, f(x_n)\right]$ is the computation matrix, which depends on the chosen experimental points and the assumed model,
- $\left({}^t XX\right)^{-1}$ is the dispersion matrix,
- $f\left(x_i\right)$ is the modeled vector for point x_i.

In this case, we define $n_1\left(x\right)$ for a configuration x as follows:

$$m_1(x) = \sum_{i=1}^{n} 1_{\text{Var}\left(\hat{y}_{x_i}\right)\leq\epsilon}$$

As a second mark, we will take the average of the normal density distances between point x_i and the other points in configuration x. This mark will be given by:

$$m_2(x) = \sum_{i=1}^{n} 1_{\mu(x_i)\leq r}$$

Where $\mu\left(x_i\right) = \frac{1}{n-1}\sum\limits_{\substack{i=1\\ j\neq i}}^{n} \delta\left(x_i, x_j\right)$ with $\delta\left(x_i, x_j\right) = \int\limits_0^l \varphi(t)dt$, where l is the usual distance between points x_i and x_j. φ represents the density of the normal distribution where ε and r are fixed values.

4. Simulation of Point Processes using the MCMC Method and the Metropolis-Hastings Algorithm

This method involves constructing a chain $\{X_0, X_1, \ldots, X_N\}$ that converges to the desired distribution π. In fact, the Metropolis-Hastings (MH) algorithm can perform this construction using the π-reversible transition kernel. Recall that the algorithm goes through two steps.

- We propose a state change from x to y according to the probability distribution $Q\left(x, \cdot\right)$,
- We accept y with probability $a(x, y)$, otherwise, we stay in the state x (Where $a : \Omega \times \Omega \mapsto [0, 1]$).

Let $q(x, y)$ be the density of $Q\left(x, \cdot\right)$, the MH transition is written as [9]:

$$P_{MH}\left(x, y\right) = a\left(x, y\right) q\left(x, y\right) + \left[1 - \int\limits_{\Omega} a\left(x, z\right) q\left(x, z\right) dz\right] \delta_x(y)$$

With $\delta_x(.)$ representing the point mass at x. To simplify calculations, we use the Dirac measure at x ($\delta_x\left(y\right) = 1$ if $x = y$ and 0 otherwise).

The choice of (Q, a) will ensure the π-reversibility of P_{MH} if the following equilibrium equation is satisfied:

$$\forall x, y \in \Omega : \ \pi\left(x\right) \times q\left(x,\ y\right) \times a\left(x,\ y\right) \ = \ \pi\left(y\right) \times q\left(y,\ x\right) \times a\left(y,\ x\right)$$

The choice of the acceptance probability $a(x, y)$ is more constrained: it is essentially dictated by the goal of (asymptotically) simulating a given probability distribution π. This is the case in the usual choice, where:

$$a\,(x,\ y)\ = \frac{\pi\,(y) \times q\,(y,\ x)}{\pi\,(x) \times q\,(x,\ y)}$$

Two important points to note. First, the calculation of $a\,(x,\ y)$ does not require any knowledge of the normalization constant of (3.1). Second, in this work, we consider the case where two configurations x and y differ by exactly one point. This is referred to as local shift dynamics, and thus, the density q is symmetric:

$$q\,(y, x) = q\,(x, y)$$

In this case, the acceptance probability reduces to:

$$a(x, y) = \frac{\pi\,(y)}{\pi(x)} = \frac{\beta_1^{m_1(y)}\beta_2^{m_2(y)}\gamma_{11}^{m_{11}(y)}\gamma_{12}^{m_{12}(y)}\gamma_{22}^{m_{22}(y)}}{\beta_1^{m_1(x)}\beta_2^{m_2(x)}\gamma_{11}^{m_{11}(x)}\gamma_{12}^{m_{12}(x)}\gamma_{22}^{m_{22}(x)}}$$

4.1. **The algorithm for constructing the proposed experiment design.** The computer experiment design proposed in this work [referred to as the two-type marked experiment design] is generated using the following algorithm:

Algorithm 1:

- **Initialization step:** Choose an initial configuration (experiment design) $\left(X_0 = x \text{ or } x = (x_1, x_2, \ldots, x_n) \text{ and } x \in [0,1]^k\right)$ according to a given probability distribution, for example, the uniform distribution.
- Iteration step:

for $N = 1, 2, ..., N_{MCMC}$ **do**

  for *each configuration* x **do**

    sample y using local shift dynamics.

    - Randomly select a spin j uniformly from the set $\{1, \cdots, n\}$.
    - Move the point x_j according to a normal distribution centered at x_j with variance r, that is, $y_j = x_j + \varepsilon$ where ε follows $N(x_j, r)$. The new configuration is then taken as:

$$y = (x_1, x_2, \cdots, x_{j-1}, y_j, x_{j+1}, \cdots, x_n).$$

  end

  - Calculation of the acceptance probability $a(x, y) = \min\left(1; \beta_1^{m_1(y)-m_1(x)}\beta_2^{m_2(y)-m_2(x)}\gamma_{11}^{m_{11}(y)-m_{11}(x)}\gamma_{12}^{m_{12}(y)-m_{12}(x)}\gamma_{22}^{m_{22}(y)-m_{22}(x)}\right)$.
  - Take $x = \begin{cases} y \text{ with a probability } a \\ x \text{ with a probability } 1-a \end{cases}$.

  Repeat these last two steps n times for each iteration N.

  Take $X_N = x$

end

For $N = 1000$, Figure 2 shows the convergence towards a configuration that characterizes the realization of a two-marked Strauss point process from an initial configuration of 50 points chosen uniformly in $[0,1]^2$:

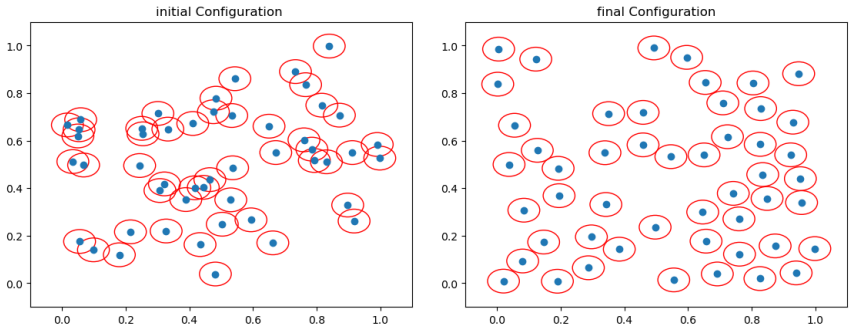

FIGURE 2. On the left, represents an initial configuration of 50 points, and on the right, a final configuration for $\gamma_{11} = 0.01$, $\gamma_{12} = 0.01$, $\gamma_{22} = 0.05$, $\beta_1 = 0.9$, $\beta_2 = 1.5$ and $r = 0.1$.

The interactions between the experiments will be shown in Figure 2 using circles with a radius of $r/2$. When two circles overlap, it indicates a specific interaction between those experiments. If the radius r is too small, the distribution shows no interactions. On the other hand, if the radius is too large, the distribution forms clusters. Therefore, it is crucial to choose an appropriate radius to avoid these issues. The value must be carefully selected. For a given criterion, the best solution would likely be to tabulate this value based on the number of points and the problem's dimension.

5. Convergence Study

For each iteration N of the construction algorithm described above, we perform n basic transformations. Therefore, the chain of experimental designs $(X_N)_{N\geq 0}$ generated in this way is the realization of a Markov chain with the transition kernel:

$$P(x,y) = P_{MH}^{n}(x,y)$$

At this point, the fundamental question is whether the chain converges to the distribution $\pi(x)$ defined in (3.1). The chain converges to the invariant distribution π if:

$$P^t(x,A) \underset{t\to\infty}{\to} \pi(A)$$

Where A is a Borel set from $\mathcal{A}$, and $P^t(x,A) = p(X_t = A/X_0 = x)$ is a transition kernel at time t. Let's state the main result of interest here:

Proposition 5.1. *On a finite space, the transition kernel P of the Markov chain $(X_N)_{N\geq 0}$ obtained from the construction algorithm is positive recurrent, π-stationary, aperiodic, and primitive (primitive Kernel).*

Proof. First, we demonstrate three important properties for the kernel P_{MH}: π-reversibility, π-stationarity, and π-irreducibility.

- π**-reversibility:** By definition, the transition P_{MH} is π-reversible if:

$$\forall x,\ y\ \in\ \Omega\ :\ \pi\left(x\right)P_{MH}\left(x,\ y\right)\ =\ \pi\left(y\right)P_{MH}\left(y,\ x\right)$$

Let $x \in \Omega$ and $B \in \mathcal{A}$, we have:

$$\int_{\Omega} 1_{B(x,y)}\pi\left(x\right)P_{MH}\left(x,y\right)dx = \int_{\Omega} 1_{B(x,y)}\pi\left(x\right)a\left(x,y\right)q\left(x,y\right)dx$$

$$+\int_{\Omega} 1_{B(x,y)}\pi\left(x\right)\left[1-\int_{\Omega} a\left(x,z\right)q\left(x,z\right)dz\right]\delta_x\left(y\right)dx$$

$$=\int_{\Omega} 1_{B(x,y)}\pi\left(x\right)a\left(x,y\right)q\left(x,y\right)dx$$

$$+\int_{\Omega} 1_{B(x,y)}\delta_x\left(y\right)\pi\left(x\right)\left[1-\int_{\Omega} a\left(x,z\right)q\left(x,z\right)dz\right]dx$$

$$=\int_{\Omega} 1_{B(x,y)}\pi\left(x\right)a\left(x,y\right)q\left(x,y\right)dx$$

$$+\int_{\Omega} 1_{B(x,x)}\pi\left(x\right)\left[1-\int_{\Omega} a\left(x,z\right)q\left(x,z\right)dz\right]dx$$

And since:

$$\pi\left(x\right)a\left(x,y\right)q\left(x,y\right)=\alpha\beta_1^{m_1(x)}\beta_2^{m_2(x)}\gamma_{11}^{m_{11}(x)}\gamma_{12}^{m_{12}(x)}\gamma_{22}^{m_{22}(x)}$$

$$\times\min\left(1;\beta_1^{m_1(y)-m_1(x)}\beta_2^{m_2(y)-m_2(x)}\gamma_{11}^{m_{11}(y)-m_{11}(x)}\gamma_{12}^{m_{12}(y)-m_{12}(x)}\gamma_{22}^{m_{22}(y)-m_{22}(x)}\right)q(x,y)$$

$$=\alpha\min\left(\beta_1^{m_1(x)}\beta_2^{m_2(x)}\gamma_{11}^{m_{11}(x)}\gamma_{12}^{m_{12}(x)}\gamma_{22}^{m_{22}(x)},\beta_1^{m_1(y)}\beta_2^{m_2(y)}\gamma_{11}^{m_{11}(y)}\gamma_{12}^{m_{12}(y)}\gamma_{22}^{m_{22}(y)}\right)q(x,y)$$

$$=\alpha\beta_1^{m_1(y)}\beta_2^{m_2(y)}\gamma_{11}^{m_{11}(y)}\gamma_{12}^{m_{12}(y)}\gamma_{22}^{m_{22}(y)}$$

$$\times\min\left(\beta_1^{m_1(x)-m_1(y)}\beta_2^{m_2(x)-m_2(y)}\gamma_{11}^{m_{11}(x)-m_{11}(y)}\gamma_{12}^{m_{12}(x)-m_{12}(y)}\gamma_{22}^{m_{22}(x)-m_{22}(y)};1\right)\times q(x,y)$$

$$=\pi(y)\min\left(1;\beta_1^{m_1(x)-m_1(y)}\beta_2^{m_2(x)-m_2(y)}\gamma_{11}^{m_{11}(x)-m_{11}(y)}\gamma_{12}^{m_{12}(x)-m_{12}(y)}\gamma_{22}^{m_{22}(x)-m_{22}(y)}\right)q(x,y)$$

$$=\pi(y)a(y,x)q(x,y)$$

And since $q\left(x,y\right)=q\left(y,x\right)$, then:

$$\pi\left(x\right)a\left(x,\ y\right)q\left(x,y\right)=\pi\left(y\right)a\left(y,x\right)q\left(y,x\right)$$

, We obtain:

$$\int_{\Omega} 1_{B(x,y)}\pi\left(x\right)P_{MH}\left(x,y\right)dx$$

$$=\int_{\Omega} 1_{B(x,y)}\pi\left(y\right)a\left(y,x\right)q\left(y,x\right)dx+\int_{\Omega} 1_{B(y,y)}\pi\left(y\right)\left[1-\int_{\Omega} a\left(y,z\right)q\left(y,z\right)dz\right]dy$$

$$= \int_{\Omega} 1_{B(x,y)} \pi(y) P_{MH}(y,x)\, dy$$

So $\pi(x) P_{MH}(x,\ y) = \pi(y) P_{MH}(y,\ x)$, and therefore, the chain is π-reversible.

- **π-stationarity:** The transition P_{MH} is π-stationary if:

$$\forall x, y \in \Omega; A, B \in \mathcal{A} : \int_{\Omega} 1_{B(x,y)} \pi(x) P_{MH}(x,A)\, dx = \int_{\Omega} 1_{B(x,y)} \pi(x)\, dx$$

Let $x \in \Omega$ and $B \in \mathcal{A}$. We then have:

$$\int_{\Omega} 1_{B(x,y)} \pi(x) P_{MH}(x,y)\, dx = \int_{\Omega} 1_{B(x,y)} \pi(x) \left[\int_{\Omega} a(x,y) q(x,y)\, dy \right] dx$$

$$+ \int_{\Omega} 1_{B(x,y)} \pi(x) \left[\int_{\Omega} 1 - a(x,z) q(x,z)\, dz \right] \delta_x(y)\, dx$$

$$= \int_{\Omega} \int_{\Omega} 1_{B(x,y)} \pi(x) a(x,y) q(x,y)\, dy dx + \int_{\Omega} 1_{B(x,x)} \pi(x)\, dx - \int_{\Omega} \int_{\Omega} \pi(x) a(x,z) q(x,z)\, dz dx$$

$$= \int_{\Omega} 1_{B(x,x)} \pi(x)\, dx$$

So the chain admits π as a stationary distribution.

- **π-irreducibility:** The transition P_{MH} is π-irreducible if:

$$\forall A \in \mathcal{A}, \pi(A) > 0 \ \Rightarrow\ \exists t\ ,\ P_{MH}^{t}(x,A) > 0$$

Let A be a Borel set from $\mathcal{A}$, and for $t = 1$ we have:

$$\int_{\Omega} 1_{B(x,A)} P_{MH}(x,A)\, dx = \int_{\Omega} 1_{B(x,A)} a(x,A) q(x,A)\, dx$$

$$+ \int_{\Omega} 1_{B(x,A)} \left[1 - \int_{\Omega} a(x,z) q(x,z)\, dz \right] \delta_x(A)\, dx$$

$$= \int_{\Omega} 1_{B(x,A)} a(x,A) q(x,A)\, dx + \int_{\Omega} 1_{B(x,x)} \left[1 - \int_{\Omega} a(x,z) q(x,z)\, dz \right] dx$$

$$= \int_{\Omega} 1_{B(x,A)} a(x,A) q(x,A)\, dx + 1 - \int_{\Omega} \int_{\Omega} a(x,z) q(x,z)\, dz dx$$

Since:

$$a(x,A) = \min\left(1; \beta_1^{m_1(A)-m_1(x)} \beta_2^{m_2(A)-m_2(x)} \gamma_{11}^{m_{11}(A)-m_{11}(x)} \gamma_{12}^{m_{12}(A)-m_{12}(x)} \gamma_{22}^{m_{22}(A)-m_{22}(x)}\right)$$

and

$$a(x,z) = \min\left(1; \beta_1^{m_1(z)-m_1(x)} \beta_2^{m_2(z)-m_2(x)} \gamma_{11}^{m_{11}(z)-m_{11}(x)} \gamma_{12}^{m_{12}(z)-m_{12}(x)} \gamma_{22}^{m_{22}(z)-m_{22}(x)}\right)$$

Then we have four possible cases:

- if $a\left(x,A\right)=1$ and

$$a(x,z)=\beta_1^{m_1(z)-m_1(x)}\beta_2^{m_2(z)-m_2(x)}\gamma_{11}^{m_{11}(z)-m_{11}(x)}\gamma_{12}^{m_{12}(z)-m_{12}(x)}\gamma_{22}^{m_{22}(z)-m_{22}(x)}$$

then:

$$\int_{\Omega}1_{B(x,A)}P_{MH}\left(x,A\right)dx=\int_{\Omega}1_{B(x,A)}q\left(x,A\right)dx+1$$

$$-\int_{\Omega}\int_{\Omega}\beta_1^{m_1(z)-m_1(x)}\beta_2^{m_2(z)-m_2(x)}\gamma_{11}^{m_{11}(z)-m_{11}(x)}\gamma_{12}^{m_{12}(z)-m_{12}(x)}\gamma_{22}^{m_{22}(z)-m_{22}(x)}q\left(x,z\right)dzdx$$

$$=\int_{\Omega}1_{B(x,A)}q\left(x,A\right)dx+1$$

$$-\beta_1^{m_1(z)-m_1(x)}\beta_2^{m_2(z)-m_2(x)}\gamma_{11}^{m_{11}(z)-m_{11}(x)}\gamma_{12}^{m_{12}(z)-m_{12}(x)}\gamma_{22}^{m_{22}(z)-m_{12}(x)}>0$$

- if $a(x,z)=\beta_1^{m_1(A)-m_1(x)}\beta_2^{m_2(A)-m_2(x)}\gamma_{11}^{m_{11}(A)-m_{11}(x)}\gamma_{12}^{m_{12}(A)-m_{12}(x)}\gamma_{22}^{m_{22}(A)-m_{22}(x)}$ and $a\left(x,z\right)=1$ then:

$$\int_{\Omega}1_{B(x,A)}P_{MH}\left(x,A\right)dx$$

$$=\int_{\Omega}1_{B(x,A)}\beta_1^{m_1(A)-m_1(x)}\beta_2^{m_2(A)-m_2(x)}\gamma_{11}^{m_{11}(A)-m_{11}(x)}\gamma_{12}^{m_{12}(A)-m_{12}(x)}\gamma_{22}^{m_{22}(A)-m_{22}(x)}q\left(x,A\right)dx$$

$$+1-\int_{\Omega}\int_{\Omega}q\left(x,z\right)dzdx$$

$$=\beta_1^{m_1(A)-m_1(x)}\beta_2^{m_2(A)-m_2(x)}\gamma_{11}^{m_{11}(A)-m_{11}(x)}\gamma_{12}^{m_{12}(A)-m_{12}(x)}\gamma_{22}^{m_{22}(A)-m_{22}(x)}\int_{\Omega}1_{B(x,A)}q\left(x,A\right)dx>0$$

- if $a(x,z)=\beta_1^{m_1(A)-m_1(x)}\beta_2^{m_2(A)-m_2(x)}\gamma_{11}^{m_{11}(A)-m_{11}(x)}\gamma_{12}^{m_{12}(A)-m_{12}(x)}\gamma_{22}^{m_{22}(A)-m_{22}(x)}$ and $a(x,z)=\beta_1^{m_1(z)-m_1(x)}\beta_2^{m_2(z)-m_2(x)}\gamma_{11}^{m_{11}(z)-m_{11}(x)}\gamma_{12}^{m_{12}(z)-m_{12}(x)}\gamma_{22}^{m_{22}(z)-m_{22}(x)}$ then:

$$\int_{\Omega}1_{B(x,A)}P_{MH}\left(x,A\right)dx$$

$$=\int_{\Omega}1_{B(x,A)}\beta_1^{m_1(A)-m_1(x)}\beta_2^{m_2(A)-m_2(x)}\gamma_{11}^{m_{11}(A)-m_{11}(x)}\gamma_{12}^{m_{12}(A)-m_{12}(x)}\gamma_{22}^{m_{22}(A)-m_{22}(x)}q\left(x,A\right)dx+1$$

$$-\int_{\Omega}\int_{\Omega}\beta_1^{m_1(z)-m_1(x)}\beta_2^{m_2(z)-m_2(x)}\gamma_{11}^{m_{11}(z)-m_{11}(x)}\gamma_{12}^{m_{12}(z)-m_{12}(x)}\gamma_{22}^{m_{22}(z)-m_{22}(x)}q\left(x,z\right)dzdx$$

$$=\beta_1^{m_1(A)-m_1(x)}\beta_2^{m_2(A)-m_2(x)}\gamma_{11}^{m_{11}(A)-m_{11}(x)}\gamma_{12}^{m_{12}(A)-m_{12}(x)}\gamma_{22}^{m_{22}(A)-m_{22}(x)}\int_{\Omega}1_{B(x,A)}q\left(x,A\right)dx+1$$

$$-\beta_1^{m_1(z)-m_1(x)}\beta_2^{m_2(z)-m_2(x)}\gamma_{11}^{m_{11}(z)-m_{11}(x)}\gamma_{12}^{m_{12}(z)-m_{12}(x)}\gamma_{22}^{m_{22}(z)-m_{22}(x)}\int_{\Omega}\int_{\Omega}q\left(x,z\right)dzdx$$

$$=\beta_1^{m_1(A)-m_1(x)}\beta_2^{m_2(A)-m_2(x)}\gamma_{11}^{m_{11}(A)-m_{11}(x)}\gamma_{12}^{m_{12}(A)-m_{12}(x)}\gamma_{22}^{m_{22}(A)-m_{22}(x)}\int_{\Omega}1_{B(x,A)}q\left(x,A\right)dx+1$$

$$-\beta_1^{m_1(z)-m_1(x)}\beta_2^{m_2(z)-m_2(x)}\gamma_{11}^{m_{11}(z)-m_{11}(x)}\gamma_{12}^{m_{12}(z)-m_{12}(x)}\gamma_{22}^{m_{22}(z)-m_{22}(x)} > 0$$

So $\int_\Omega 1_{B(x,A)} {P_{MH}}^t (x, A)\, dx > 0 \;\forall\; t \geq 0$, then P_{MH}est π-irreducible.

Since π is the invariant distribution of P_{MH}, it is also an invariant distribution for P. Indeed, $\pi P_{MH} = \pi$, and by induction on the integer, $\pi P_{MH} = \pi$, we obtain:

$$\pi P_{MH} = \pi P_{MH}^2 = \pi P_{MH}^3 = \ldots = \pi P_{MH}^n = \pi$$

So, $\pi P = \pi$. By construction of $P = P_{MH}^n$, the π-irreducibility of P_{MH} implies the π-irreducibility of P. If P is π-irreducible and has an invariant distribution π, then P is positive recurrent, and π is the unique invariant distribution of P. By construction of $P = P_{MH'}^n$ we have $\pi P = \pi$. If P is π-irreducible and has an invariant distribution π, then P is positive recurrent, and π is the unique invariant distribution of P [9] (see proposition 1).

Furthermore, the chain created by the construction algorithm will also be aperiodic as long as there exists at least one pair of configurations (x, y) such that $a(x, y) < 1$, because then we have $P(x, x) > 0$. It is quickly evident that the chain is aperiodic, as the event $X_{(N+1)} = X_{(N)}$ is possible practically at any time. Indeed, each state can be visited in two consecutive iterations, so $P^1(x, x) > 0$, making their period 1.

Since the chain generated by the algorithm is irreducible and aperiodic, its transition kernel P is primitive (a characterization of a primitive Markov Kernel more common in probability theory is to say that it is irreducible and aperiodic). □

Theorem 5.1. *The Markov chain $(X_N)_{N \geq 0}$ obtained from the proposed construction algorithm is geometrically ergodic, and its kernel P simulates a marked point process with two types of density:*

$$\pi(x) = \alpha\beta_1^{m_1(x)}\beta_2^{m_2(x)}\gamma_{11}^{m_{11}(x)}\gamma_{12}^{m_{12}(x)}\gamma_{22}^{m_{22}(x)}$$

In other words, vP^m converges to π as m tends to infinity, where v is the initial distribution, and we have:

$$\lim_{m\to\infty} \|vP^m - \pi\| = 0$$

Proof. Let v be an initial distribution, for any integer m and for all $x \in N^{lf}$, we have:

$$\left\|vP^m(x, .) - \pi\right\| = \|vP^m - \pi P^m\| \leq 2C(P^m) \leq 2(C(P))^m$$

Where $C(P)$ is the Dobrushin contraction coefficient of P [10].

According to Proposition 1, the kernel P is primitive, so $0 \leq C(P) < 1$ [11] (see lemma 4.2.3 p.72). Therefore, as m tends to infinity, $\|vP^m - \pi\| \underset{m\to\infty}{\to} 0$. Thus, the chain is uniformly ergodic and converges to the distribution defined in (3.1). □

6. Numerical Results and Quality of the Proposed Designs

In this section, we will conduct a comparison of the point distributions in the proposed computer experiment design using established criteria. This evaluation aims to assess the effectiveness of the experimental space coverage and the uniformity of point distribution.

The criteria used for this comparison include:

- **Minimum Distance Criterion (Mindist)** [12]: This criterion aims to maximize the minimum distance between any two points in the design. The larger the minimum distance, the more evenly spread the points are, leading to better space coverage.

$$Mindist = \min_i \min_{j \neq i} d(x_i, x_j)$$

where $d(x_i, x_j)$ represents the Euclidean distance between points x_i and x_j. A higher value of *Mindist* indicates a more regular dispersion of points.

- **Discrepancy Criterion (Disc)** [13]: The discrepancy measures the difference between the empirical distribution of the points in the design and a uniform distribution. Unlike the previous criterion, discrepancy does not rely on the distance between points but instead evaluates how well the points approximate a uniform distribution. We use the L_2-norm discrepancy.

$$Disc = \left(\frac{1}{3}\right)^p - \frac{2^{1-p}}{n} \sum_{i=1}^{n} \prod_{j=1}^{p} \left(1 - \left(x_i^j\right)^2\right) + \frac{1}{n^2} \sum_{i=1}^{n} \sum_{k=1}^{n} \prod_{j=1}^{p} \left(1 - \max\left(x_i^j, x_k^j\right)\right)$$

A lower discrepancy value indicates that the points are closer to a uniform distribution.

- **Coverage Criterion (Cov)** [14]: This criterion measures the difference between the points of the design and those of a regular grid. For a perfect regular grid, this criterion is zero. The goal is to minimize the coverage criterion to approach a regular grid, while still maintaining a uniform distribution, especially when projected onto factorial axes:

$$Cov = \frac{1}{\bar{\delta}} \sqrt{\frac{1}{n} \sum_{i=1}^{n} \left(\delta_i - \bar{\delta}\right)^2}$$

where $\delta_i = \min_{i \neq j} d(x_i, x_j)$ and $\bar{\delta} = \frac{1}{n} \sum_{i=1}^{n} \delta_i$. A lower coverage value implies that the points are closer to a regular grid, ensuring effective space-filling while maintaining uniformity.

- R **Criterion**: The R criterion is the ratio between the maximum and minimum distance between points in the experimental design. For a perfect regular grid, $R = 1$. Thus, the closer R is to 1, the closer the points are to a regular grid:

$$R = \frac{\max\limits_{i \in \{1,\ldots,n\}} \delta_i}{\min\limits_{i \in \{1,\ldots,n\}} \delta_i}$$

where $\delta_i = \min_{i \neq j} d(x_i, x_j)$. A value of R closer to 1 suggests that the points are more equidistant, promoting a more regular distribution.

The Table 1 presents a comparison based on the discrepancy criterion between the plans proposed in this work (denoted TMD: Two Mark Designs) and low-discrepancy sequences (Halton sequence [15], Sobol sequence [16], and Faure sequence [17]). It is interesting to observe that the proposed plans have low discrepancy, comparable to that of low-discrepancy sequences.

In this article, the constructed designs are also compared with commonly used designs in computer experiments, excluding low-discrepancy sequences. To provide meaningful results, the

TABLE 1. The values of discrepancy for the proposed designs TMD, Halton sequences, Sobol sequences and faure sequence for different dimensions.

Number of Factors	Number of Points	TMD	Halton Sequence	Sobol Sequence	Faure Sequence
4	32	0.0016252	0.001779	0.000843	0.001641
7	64	0.00009093	0.00048	0.000224	0.000480
10	128	0.000004925	0.000109	0.0000605	0.000109

comparison criteria were computed for a set of 80 distinct designs. This ensures a robust and thorough evaluation of the different methodologies in terms of quality and efficiency. The designs analyzed in this section are as follows:

- **Random Designs (RD)**: These designs are generated by distributing points according to a uniform distribution over the hypercube $[0,1]^p$, ensuring a random distribution in the parameter space.
- **Latin Hypercube Designs (LH)**: LH designs are experimental design techniques that aim to sample the parameter space efficiently and uniformly, optimizing the coverage of the studied dimensions [18].
- **Maximin Latin Hypercube Designs (mLHS)**: These optimal designs are based on the Maxmin criterion, which seeks to maximize the minimum distance between points in the design space, ensuring better dispersion of the points [19].
- **Maximum Entropy Designs (Dmax)**: Designs constructed to maximize the determinant of a covariance matrix. These designs are often employed in kriging to fit response surfaces, assuming an underlying model [20].
- **Strauss Designs (SD)**: These designs, derived from a Strauss process, incorporate repulsion between points to optimize the coverage of the parameter space [2].
- **Marked Strauss Designs**: These designs are generated from a marked Strauss process, incorporating point repulsion and associating each point with a specific mark to minimize the prediction error function [3].
- **Connected Component Designs (CCD)**: These designs are developed from a Markov point process with connected components, characterized by more or less regular spatial distributions without constraints on the parameters [5].
- **Proposed Designs (TMD)**.

Figures 3,4 and 5 highlight several important points. Among the evaluated design methods, maximum entropy designs, Latin hypercube sampling (LHS) designs, Maximin Latin hypercube designs, connected component designs, and Two-Type designs all achieve favorable results based on the discrepancy criterion. It is fascinating that Two-Type designs, which are part of this list, also stand out for their excellent performance according to the R-criterion. This dual satisfaction of both

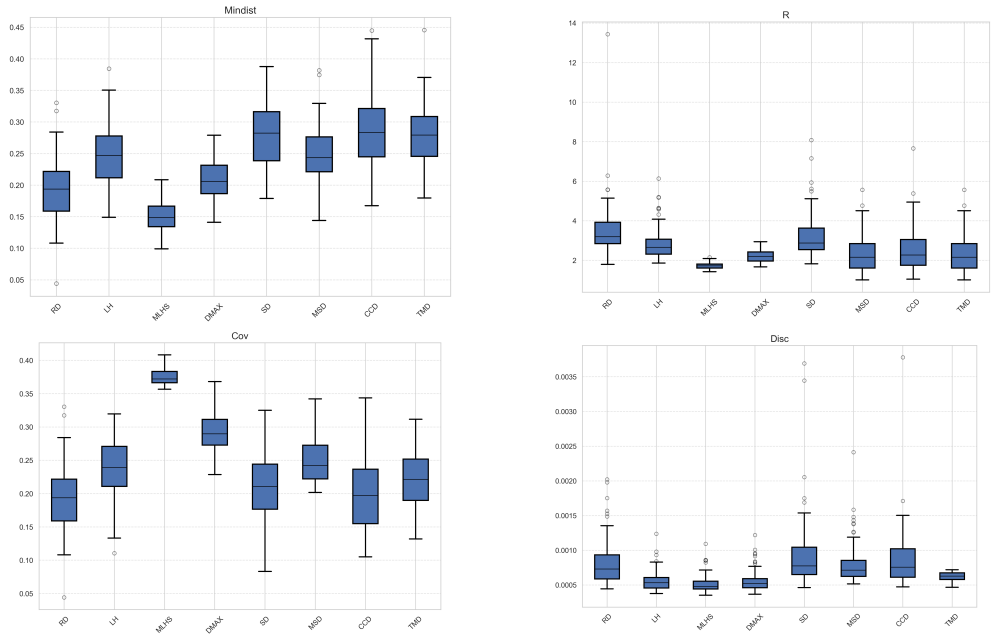

FIGURE 3. Box plots of quality criteria calculated for 100 designs with 30 points in 5 dimensions

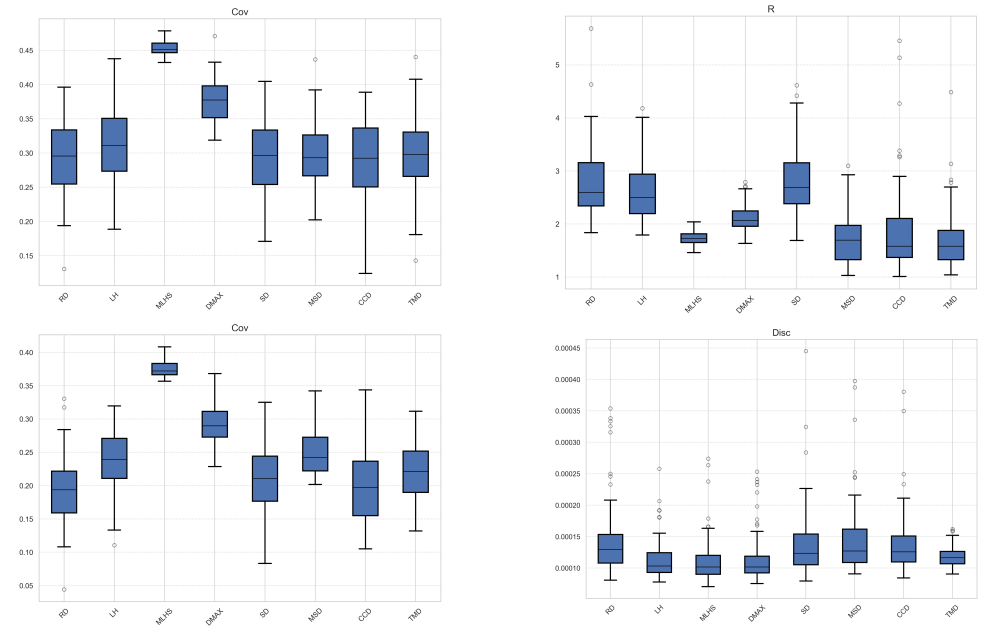

FIGURE 4. Box plots of quality criteria calculated for 100 designs with 50 points in 7 dimensions.

criteria by Two-Type designs underscores their robustness and efficiency in various experimental scenarios. It reinforces the idea that adapting designs to specific evaluation criteria is essential for optimizing overall experimental performance.

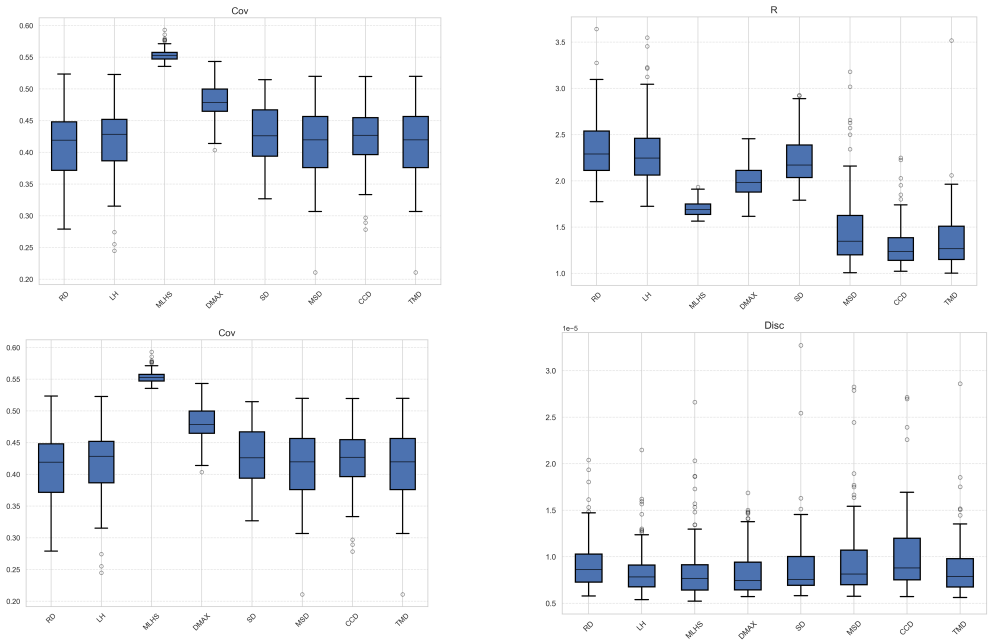

FIGURE 5. Box plots of quality criteria calculated for 100 designs with 100 points in 10 dimensions.

7. CONCLUSION

The design of the experiment method provides a powerful and versatile framework for experimenters across various fields to plan and optimize their experimental processes. By integrating two-type marked point processes with the Markov Chain Monte Carlo (MCMC) method, researchers can now develop innovative designs for computer experiments that are informed by the underlying principles of pairwise interaction models. This combination not only enhances the precision and adaptability of the experimental setup but also offers substantial flexibility. The ability to manipulate the law governing the interaction model, for example by enforcing specific properties like space-filling, opens up new possibilities for fine-tuning experiment designs. Consequently, this approach provides a robust tool for experimenters aiming to refine their models, ensuring more accurate, reliable, and insightful results in complex experimental scenarios.

Conflicts of Interest: The authors declare that there are no conflicts of interest regarding the publication of this paper.

REFERENCES

[1] B.D. Ripley, F.P. Kelly, Markov Point Processes, J. Lond. Math. Soc. s2-15 (1977), 188–192. https://doi.org/10.1112/jlms/s2-15.1.188.

[2] J. Franco, Planification d'Expériences Numériques en Phase Exploratoire pour des Codes de Calculs Simulant des Phénomènes Complexes, Doctoral Thesis, l'Ecole Nationale Supérieure des Mines de Saint-Etienne, France, (2008).

[3] H. Elmossaoui, N. Oukid, F. Hannane, Construction of Computer Experiment Designs Using Marked Point Processes, Afr. Mat. 31 (2020), 917–928. https://doi.org/10.1007/s13370-020-00770-9.

[4] H. Elmossaoui, Contribution à la Méthodologie de la Recherche Expérimentale, Doctoral Thesis, University Saad Dahleb, Blida, Algerie, (2020).

[5] H. Elmossaoui, N. Oukid, New Computer Experiment Designs Using Continuum Random Cluster Point Process, Int. J. Anal. Appl. 21 (2023), 51. https://doi.org/10.28924/2291-8639-21-2023-51.

[6] A. Ait Ameur, H. Elmossaoui, N. Oukid, New Computer Experiment Designs with Area-Interaction Point Processes, Mathematics 12 (2024), 2397. https://doi.org/10.3390/math12152397.

[7] A. Baddeley, J. Møller, J. Moller, Nearest-Neighbour Markov Point Processes and Random Sets, Int. Stat. Rev. 57 (1989), 89-121. https://doi.org/10.2307/1403381.

[8] W.K. Hastings, Monte Carlo Sampling Methods Using Markov Chains and Their Applications, Biometrika 57 (1970), 97–109. https://doi.org/10.1093/biomet/57.1.97.

[9] S. Chib, E. Greenberg, Understanding the Metropolis-Hastings Algorithm, Amer. Stat. 49 (1995), 327–335. https://doi.org/10.1080/00031305.1995.10476177.

[10] R.L. Dobrushin, Central Limit Theorem for Nonstationary Markov Chains. I, Theor. Probab. Appl. 1 (1956), 65–80. https://doi.org/10.1137/1101006.

[11] G. Winkler, Image Analysis Random fields and Dynamic Monte Carlo Methods, Springer, Berlin, (1995).

[12] M. Gunzburger, J. Burkardt, Uniformity Measures for Point Samples in Hypercubes, (2004). https://people.sc.fsu.edu/~jburkardt/publications/gb_2004.pdf.

[13] T.T. Warnock, Computational Investigations of Low-Discrepancy Point Sets II, in: H. Niederreiter, P.J.-S. Shiue (Eds.), Monte Carlo and Quasi-Monte Carlo Methods in Scientific Computing, Springer New York, 1995: pp. 354–361. https://doi.org/10.1007/978-1-4612-2552-2_23.

[14] M.E. Johnson, L.M. Moore, D. Ylvisaker, Minimax and Maximin Distance Designs, J. Stat. Plan. Inference 26 (1990), 131–148. https://doi.org/10.1016/0378-3758(90)90122-B.

[15] J.H. Halton, On the Efficiency of Certain Quasi-Random Sequences of Points in Evaluating Multi-Dimensional Integrals, Numer. Math. 2 (1960), 84–90. https://doi.org/10.1007/BF01386213.

[16] I.M. Sobol, Uniformly Distributed Sequences with an Additional Uniform Property, USSR Comput. Math. Math. Phys. 16 (1976), 236–242. https://doi.org/10.1016/0041-5553(76)90154-3.

[17] H. Faure, Discrépance de Suites Associées à Un Système de Numération (En Dimension s), Acta Arith. 41 (1982), 337–351. https://doi.org/10.4064/aa-41-4-337-351.

[18] W.-L. Loh, On Latin Hypercube Sampling, Ann. Stat. 24 (1996), https://doi.org/10.1214/aos/1069362310.

[19] M.D. Morris, T.J. Mitchell, Exploratory Designs for Computational Experiments, J. Stat. Plan. Inference 43 (1995), 381–402. https://doi.org/10.1016/0378-3758(94)00035-T.

[20] M.C. Shewry, H.P. Wynn, Maximum Entropy Sampling, J. Appl. Stat. 14 (1987), 165–170. https://doi.org/10.1080/02664768700000020.